

Replica study of pinned bubble crystals

R. Côté,¹ Mei-Rong Li,¹ A. Faribault,¹ and H. A. Fertig²

¹Département de physique and RQMP, Université de Sherbrooke, Sherbrooke, Québec, Canada, J1K 2R1

²Department of Physics, Indiana University, Bloomington, Indiana 47405

(Dated: November 19, 2018)

In higher Landau levels ($N > 1$), the ground state of the two-dimensional electron gas in a strong perpendicular magnetic field evolves from a Wigner crystal for small filling ν of the partially filled Landau level, into a succession of bubble states with increasing number of guiding centers per bubble as ν increases, to a modulated stripe state near $\nu = 0.5$. In this work, we compute the frequency-dependent longitudinal conductivity $\sigma_{xx}(\omega)$ of the Wigner and bubble crystal states in the presence of disorder. We apply an elastic theory to the crystal states which is characterized by a shear and a bulk modulus. We obtain both moduli from the microscopic time-dependent Hartree-Fock approximation. We then use the replica and Gaussian variational methods to handle the effects of disorder. Within the semiclassical approximation we get the dynamical conductivity as well as the pinning frequency as functions of the Landau level filling factor and compare our results with recent microwave experiments.

PACS numbers: 73.43.-f, 73.20.Qt, 73.21.-b

I. INTRODUCTION

In the presence of a strong quantizing magnetic field, the two-dimensional electron gas (2DEG) is expected to crystallize below a filling factor $\nu \sim 1/6.5$.¹ The resulting electron solid, or Wigner crystal (WC), has been intensively studied, theoretically, since the early days of the quantum Hall effect. On the experimental side, many groups have reported the observation of a strong increase in the diagonal resistivity ρ_{xx} together with non-linear I-V characteristics and broadband noise when the filling factor of the lowest Landau level is decreased below 1/5. These observations have been interpreted as the pinning and sliding of a Wigner crystal.² Early microwave absorption experiments³ detected a resonance in the real part of the longitudinal conductivity tensor, $\sigma_{xx}(\omega)$, that was attributed to the formation of a pinned Wigner crystal. (A more recent experiment⁴ reports the observation of not one but two resonances at low filling factor. The origin of these resonances are not yet fully understood.) More recent studies show a resonance in the absorption at filling factors close to $\nu = 1, 2, 3$ where the formation of a Wigner solid is expected in very clean samples.^{5,6}

In this paper, we concern ourselves with a series of microwave absorption experiments⁷ on the so-called bubble phases in Landau levels $N = 2$. The bubble phases, first introduced by Fogler and Koulakov,⁸ are basically crystals made of clusters of M electrons. More precisely, the guiding centers of the cyclotron motion (the cyclotron radius is given by $R_c = \sqrt{2N+1}\ell$ where $\ell = \sqrt{\hbar c/eB}$ is the magnetic length) of the M electrons are concentrated in a small area of radius $R_M = \sqrt{2M}\ell$ at each lattice site. In the Hartree-Fock approximation, the 2DEG ground state, in Landau levels $N > 1$, evolves from a Wigner crystal ($M = 1$), near integer filling, into bubble crystals with $M = 2, \dots, N+1$ as the filling factor increases, and terminates with the quantum Hall stripe state near half-filling of the partially filled level¹⁰. (The sequence repeats in inverse order for holes for partial filling factors between 0.5 and 1.0.) All these transitions are believed to be first order.

Microwave absorption experiments⁷ reveal a resonance in the second Landau level ($N = 2$) near integer filling, which was attributed to the formation of a Wigner crystal. The frequency of this resonance decreases, as the filling factor $\nu = \nu_{tot} - 2N$ of the partially filled level increases, until it reaches a plateau at $\nu = \nu_1 \approx 0.16$ where a second resonance appears (see Fig. 3 of Ref. 7). This second resonance is attributed to the formation of a bubble crystal with $M = 2$. The frequencies of both resonances are nearly constant between ν_1 and $\nu_2 \approx 0.26$. At ν_2 , the first resonance disappears and the frequency of the second one starts to decrease. It has been suggested that the presence of the two resonances between ν_1 and ν_2 can be explained by the coexistence of the two crystal phases in this range of filling factor.⁹

In a recent paper, we have studied the dynamics of the bubble crystals in the absence of disorder¹⁰. We have shown that these crystals have a low-energy magnetophonon mode with dispersion $\omega \sim k^{3/2}$, at small wavevector, that is typical of a pure Wigner crystal in a strong magnetic field. In the presence of disorder, this low-energy magnetophonon mode becomes gapped, with lowest energy at the pinning frequency. In this paper, we compute this pinning frequency and the evolution of the longitudinal part of the dynamical conductivity, $\sigma_{xx}(\omega)$, as the 2DEG makes transitions from the WC to the bubble states and compare our results with those of Lewis et al.⁷ (We have previously addressed the dynamics of the disordered stripe state in Refs. 11 and 12). The pinning frequency is extracted from the real

part of the dynamical conductivity *i.e.* from $\Re[\sigma_{xx}(\mathbf{q} = 0, \omega)]$ computed in the presence of disorder. To deal with the disorder averaging, we use a combination of the replica trick and Gaussian variational methods (GVM).¹³ A similar technique has been used by Chitra *et al.*¹⁴ to compute the dynamical conductivity tensor of the Wigner crystal in the lowest Landau level. While this method appears to give reasonable results for this and other pinned systems, some controversy has arisen regarding the width of the resulting resonant peak for a pinned Wigner crystal in a magnetic field^{15,16}. We address this issue toward the end of this paper.

To deal with the bubble crystals, some modifications of the replica method are needed. For example, electrons and bubbles are more extended objects in higher Landau levels and so it is necessary to include a form factor in the calculation of the dynamical matrix that enters the elastic action as well as the effective disorder potential. We find that the evolution of the bulk and shear moduli with filling factor is essentially driven by the changes in the form factor of the bubbles. A softening of the lattice appears at the critical filling ν_1 introduced above when the outer radii of adjacent bubbles touch one another and, as we will show, is correctly captured by a dynamical matrix computed with the correct form factor. Moreover, the gap between the two pinning resonances seen in the microwave experiment may be understood as being partially due to the change in form factor in the transition from the Wigner to the $M = 2$ bubble crystal. In our calculation, the bulk and shear moduli are extracted from the density-density response function computed in the Generalized-Random-Phase Approximation (GRPA).¹⁹

Our paper is organized in the following way. In Sec. II, we build an elastic model for the description of the pure crystal states and extract the dynamical matrix from the GRPA calculation. In Sec. III, we briefly review the replica and GVM that we use to handle the disorder. Our numerical results for the dynamical conductivity and pinning peak are presented in Sec. IV. We compare our results with the experimental data in Sec. V. Section VI is devoted to a discussion of the width of the resonance obtained in this method as compared to others, and we conclude with a summary in Sec. VII. A brief account of this work has appeared previously.¹⁸

II. ELASTIC MODEL FOR THE BUBBLE CRYSTALS

A. Form factor

In describing the bubble crystals in higher Landau levels, we assume, as usual, that the electrons in the filled levels are inert. The electrons in the partially filled Landau level N are assumed to form a triangular crystal structure¹⁰ with M electrons associated with each lattice site. It is convenient to describe the crystal by the Fourier components $\langle \rho(\mathbf{K}) \rangle$ of the guiding-center density where \mathbf{K} is a reciprocal lattice vector of the triangular lattice. The guiding center density is related to the real electronic density¹⁰ by the relation

$$\langle n(\mathbf{K}) \rangle = \int d\mathbf{r} e^{-i\mathbf{K} \cdot \mathbf{r}} \langle n(\mathbf{r}) \rangle = N_\varphi F_N(\mathbf{K}) \langle \rho(\mathbf{K}) \rangle, \quad (1)$$

where $\langle n(\mathbf{K}) \rangle$ is a Fourier component of the real density, N_φ is the Landau-level degeneracy, and

$$F_N(\mathbf{K}) = e^{-K^2 \ell^2 / 4} L_N^0 \left(\frac{K^2 \ell^2}{2} \right) \quad (2)$$

($L_N^0(x)$ is a generalized Laguerre polynomial) is the form factor of an electron in Landau level N .

The Hartree-Fock energy per electron in the partially filled Landau level is given by

$$\frac{E}{N} = \frac{1}{2\nu} \sum_{\mathbf{K}} [H(\mathbf{K})(1 - \delta_{\mathbf{K},0}) - X(\mathbf{K})] |\langle \rho(\mathbf{K}) \rangle|^2, \quad (3)$$

where $\nu = \nu_{tot} - 2N$ is the filling factor of the partially filled level. The Hartree and Fock interactions in Landau level N are given by

$$H_N(\mathbf{q}) = \left(\frac{e^2}{\kappa \ell} \right) \frac{1}{q \ell} e^{-\frac{q^2 \ell^2}{2}} \left[L_N^0 \left(\frac{q^2 \ell^2}{2} \right) \right]^2, \quad (4)$$

$$X_N(\mathbf{q}) = \left(\frac{e^2}{\kappa \ell} \right) \sqrt{2} \int_0^\infty dx e^{-x^2} [L_N^0(x^2)]^2 J_0(\sqrt{2}xq\ell), \quad (5)$$

where κ is the dielectric constant of the host material. Figure 1 shows the Hartree-Fock energy per particle for the bubble crystals in $N = 2$. The first order transition from the WC to the $M = 2$ bubble phase occurs at $\nu_1 = 0.22$, that

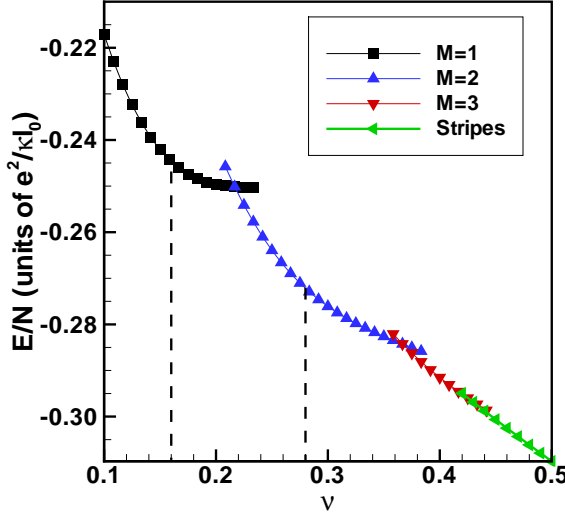


FIG. 1: Energy per particle for the bubble and stripe states in Landau level $N = 2$. The region between the dashed lines is where the two resonances are observed to coexist in the microwave experiment.

between the $M = 2$ and $M = 3$ bubble phases occurs at $\nu_2 = 0.37$ and that to the stripe phase occurs at $\nu_3 = 0.43$. In Fig. 1, the energy is in units of $e^2/\kappa\ell_0$ where ℓ_0 is the magnetic length evaluated at filling factor $\nu_0 = 0.1$ using

$$\frac{e^2}{\kappa\ell} = \sqrt{\frac{2N + \nu_0}{2N + \nu}} \left(\frac{e^2}{\kappa\ell_0} \right), \quad (6)$$

an expression that takes into account the filled Landau levels. It is important to notice that the variation of the magnetic length ℓ through the $M = 1$ or $M = 2$ bubble phases is quite small for $N = 2$ so that we can effectively consider the variation of the filling factor to be equivalent to a variation of the density of electrons. In the microwave experiments⁷, two resonances are observed in the region bounded by the dashed lines in Fig. 1, which is argued to be the signature of the coexistence of the two phases.

Once the $\langle \rho(\mathbf{K}) \rangle'$'s are known in the HFA, it is possible to compute the Matsubara two-particle Green's function

$$\chi_{\mathbf{K}, \mathbf{K}'}^{(\rho, \rho)}(\mathbf{k}, \tau) = -N_\varphi \langle \mathcal{T}_\tau \tilde{\rho}(\mathbf{k} + \mathbf{K}, \tau) \tilde{\rho}(-\mathbf{k} - \mathbf{K}', 0) \rangle, \quad (7)$$

in the GRPA¹⁹. In Eq. (7), $\tilde{\rho} \equiv \rho - \langle \rho \rangle$, \mathbf{k} is a wavevector in the first Brillouin zone of the triangular lattice and \mathcal{T}_τ is the time-ordering operator. The analytical continuation $\chi_{\mathbf{K}, \mathbf{K}'}^{(\rho, \rho)}(\mathbf{k}, \omega + i\delta)$ of this Green's function gives the density response function whose poles are the collective (density) excitations of the crystal. The lowest-energy collective mode is the magnetophonon mode. We can get its dispersion relation, $\omega_{GRPA}(\mathbf{k})$ by following the lowest-energy pole with non-vanishing weight of $\chi_{\mathbf{K}=\mathbf{0}, \mathbf{K}'=\mathbf{0}}^{(\rho, \rho)}(\mathbf{k}, \omega + i\delta)$ as \mathbf{k} is varied in the Brillouin zone.

In order to compute the dynamical conductivity $\sigma_{xx}(\omega)$ of the disordered bubble crystals using the replica and GVM, it is convenient to construct an elastic theory valid for the low-energy excitations. As has been demonstrated in Refs. 11,12, we can do so by proceeding in the following way. We model the crystals as being made of rigid extended objects centered on each lattice site \mathbf{R} with a density profile (or form factor) given by $h(\mathbf{r})$. Because each bubble has M electrons, we have the normalisation

$$\int d\mathbf{r} h(\mathbf{r}) = M. \quad (8)$$

The dynamics of these objects is described by the displacement fields $\mathbf{u}(\mathbf{R}, t)$ at each lattice site \mathbf{R} . The electronic density can therefore be given by

$$n(\mathbf{r}, t) = \sum_{\mathbf{R}} h(\mathbf{r} - \mathbf{R} - \mathbf{u}(\mathbf{R}, t)). \quad (9)$$

In the ground state, the HF energy given by Eq. (3) is very well reproduced if we use the form factors⁸,

$$h(\mathbf{q}) = \int d\mathbf{r} e^{-i\mathbf{q}\cdot\mathbf{r}} h(\mathbf{r}) = e^{-q^2\ell^2/2}, \quad (10)$$

for the WC in $N = 0$ and by

$$h(\mathbf{q}) = \begin{cases} e^{-q^2\ell^2/2} \left(1 - (q\ell)^2 + \frac{1}{8}(q\ell)^4\right), & \text{for } M = 1 \\ e^{-q^2\ell^2/2} \left(2 - \frac{1}{2}(q\ell)^2\right) \left(1 - (q\ell)^2 + \frac{1}{8}(q\ell)^4\right), & \text{for } M = 2 \end{cases} \quad (11)$$

for the bubble crystals in $N = 2$. These form factors are obtained from the Slater determinant for the wavefunction of a bubble of M electrons in Landau level N

$$\Psi_N(\mathbf{r}_1, \mathbf{r}_2, \dots, \mathbf{r}_M) = \begin{vmatrix} \varphi_{N,0}(\mathbf{r}_1) & \varphi_{N,0}(\mathbf{r}_2) & \dots & \varphi_{N,0}(\mathbf{r}_M) \\ \varphi_{N,1}(\mathbf{r}_1) & \varphi_{N,1}(\mathbf{r}_2) & \dots & \varphi_{N,1}(\mathbf{r}_M) \\ \vdots & \vdots & \vdots & \vdots \\ \varphi_{N,M-1}(\mathbf{r}_1) & \varphi_{N,M-1}(\mathbf{r}_2) & \dots & \varphi_{N,M-1}(\mathbf{r}_M) \end{vmatrix}, \quad (12)$$

where $\varphi_{N,m}(\mathbf{r}) = C_{N,m} \left(\frac{r}{\ell}\right)^{|m-N|} e^{-r^2/4\ell^2} e^{i(N-m)\theta} L_{(N+m-|m-N|)/2}^{|m-N|} \left(\frac{r^2}{2\ell^2}\right)$ is the normalized wave function of an electron in the symmetric gauge $\mathbf{A} = (-B_0 y/2, B_0 x/2, 0)$ with angular momentum m . The associated one-particle density is simply

$$h(\mathbf{r}) = \left[\prod_{i=2}^M \int d\mathbf{r}_i \right] |\Psi_N(\mathbf{r}, \mathbf{r}_2, \dots, \mathbf{r}_M)|^2 = \sum_{m=0}^{m=M-1} |\varphi_{N,m}(\mathbf{r})|^2. \quad (13)$$

In the presence of a transverse magnetic field $\mathbf{B} = -B_0 \hat{\mathbf{z}}$, the equation of motion for the displacement field of the rigid object of charge Me and mass Mm^* on site i is given by

$$(Mm^*) \frac{d^2 \mathbf{u}(\mathbf{R}_i, t)}{dt^2} = \frac{MeB_0}{c} \frac{d\mathbf{u}(\mathbf{R}_i, t) \times \hat{\mathbf{z}}}{dt} - \sum_j \hat{D}(\mathbf{R}_i - \mathbf{R}_j) \cdot \mathbf{u}(\mathbf{R}_j, t), \quad (14)$$

where $\hat{D}(\mathbf{R}_i - \mathbf{R}_j)$ is the dynamical matrix of the crystal (we use a “hat” to indicate that a quantity is a 2×2 matrix). The dynamics in the strong-magnetic field limit is obtained by setting $m^* = 0$ in Eq. (14) so that, after Fourier transforming, we get

$$\frac{M\hbar}{\ell^2} \frac{d\mathbf{u}(\mathbf{k}, t)}{dt} \times \hat{\mathbf{z}} - \hat{D}(\mathbf{k}) \cdot \mathbf{u}(\mathbf{k}, t) = 0, \quad (15)$$

where we have defined

$$\hat{D}(\mathbf{R}_i - \mathbf{R}_j) = \frac{1}{N_s} \sum_{\mathbf{k}} \hat{D}(\mathbf{k}) e^{i\mathbf{k} \cdot (\mathbf{R}_i - \mathbf{R}_j)}, \quad (16)$$

and

$$\mathbf{u}(\mathbf{k}, t) = \frac{1}{\sqrt{N_s}} \sum_{\mathbf{R}} e^{-i\mathbf{k} \cdot \mathbf{R}} \mathbf{u}(\mathbf{R}, t), \quad (17)$$

with N_s the number of lattice sites. Fourier transforming in time $\mathbf{u}(\mathbf{k}, t) = \int \frac{d\omega}{2\pi} e^{i\omega t} \mathbf{u}(\mathbf{k}, \omega)$, we have, in matrix form

$$\begin{pmatrix} D_{xx}(\mathbf{k}) & D_{xy}(\mathbf{k}) - i\frac{\hbar M}{\ell^2}\omega \\ D_{yx}(\mathbf{k}) + i\frac{\hbar M}{\ell^2}\omega & D_{yy}(\mathbf{k}) \end{pmatrix} \begin{pmatrix} u_x(\mathbf{k}, \omega) \\ u_y(\mathbf{k}, \omega) \end{pmatrix} = \begin{pmatrix} 0 \\ 0 \end{pmatrix}. \quad (18)$$

Using Eq. (18), we get for the magnetophonon dispersion relation

$$\omega = \frac{\ell^2}{\hbar M} \sqrt{\det \left[\hat{D}(\mathbf{k}) \right]}. \quad (19)$$

B. Euclidean Elastic Action

Using Eq. (18), we can now write the Euclidean action S_0 of the elastic model for the pure bubble crystal. We have

$$S_0 = \frac{1}{2T} \sum_{\mathbf{k}, \omega_n} \sum_{\alpha, \beta=x, y} u_\alpha(\mathbf{k}, \omega_n) G_{\alpha\beta}^{(0)-1}(\mathbf{k}, \omega_n) u_\beta(-\mathbf{k}, -\omega_n), \quad (20)$$

where the displacement fields obey the single Landau level dynamics²³

$$[u_x(\mathbf{R}), u_y(\mathbf{R}')] = i\ell^2 \delta_{\mathbf{R}, \mathbf{R}'}. \quad (21)$$

From now on, we set $k_B = \hbar = 1$. In Eq. (20), T is the temperature, $\omega_n = 2\pi n/T$ is the bosonic Matsubara frequency, and the displacement Green's function $G_{\alpha\beta}^{(0)}(\mathbf{k}, i\omega_n) = \int_0^{1/T} d\tau e^{i\omega_n \tau} \langle \mathcal{T}_\tau u_\alpha(\mathbf{k}, \tau) u_\beta(-\mathbf{k}, 0) \rangle_{S_0}$ is related to the dynamical matrix by

$$\hat{G}^{(0)}(\mathbf{k}, i\omega_n) = \frac{\ell^4}{M^2(\omega_n^2 + \omega_\mathbf{k}^2)} \begin{pmatrix} D_{yy}(\mathbf{k}) & \frac{M\omega_n}{\ell^2} - D_{xy}(\mathbf{k}) \\ -\frac{M\omega_n}{\ell^2} - D_{yx}(\mathbf{k}) & D_{xx}(\mathbf{k}) \end{pmatrix}. \quad (22)$$

Once the Green's function has been determined in the presence of disorder, we can easily compute the conductivity. Since the electric current is carried by the charge, the current density can be expressed as:

$$\mathbf{j}(\mathbf{k}, \tau) = i \frac{Me}{v_c} \frac{d\mathbf{u}(\mathbf{k}, \tau)}{d\tau}. \quad (23)$$

The conductivity is then determined by the Kubo formula to be

$$\begin{aligned} \sigma_{\alpha\beta}(\omega) &= -\frac{1}{\omega S} \left[\int_0^{1/T} d\tau e^{i\omega_n \tau} \langle j_\alpha(\mathbf{k}=0, \tau) j_\beta(\mathbf{k}=0, 0) \rangle \right]_{i\omega_n \rightarrow \omega + i0^+} \\ &= -\frac{M^2 e^2}{v_c} i\omega G_{\alpha\beta}^{\text{ret}}(\mathbf{k}=0, \omega), \end{aligned} \quad (24)$$

where S is the area of the 2DEG and v_c is the unit cell of the bubble crystal. Since $\hat{D}(\mathbf{k}=0)=0$, it is easy to check using Eqs. (22) and (24) that, in the pure limit and in the strong magnetic field approximation, the electromagnetic response of the system is purely transverse for all frequencies $\omega \ll \omega_c$; *i.e.*, we have in this limit

$$\hat{\sigma}(\omega) = \begin{pmatrix} 0 & \frac{nec}{B} \\ -\frac{nec}{B} & 0 \end{pmatrix}, \quad (25)$$

where $n = M/\nu_c$ is the electronic density. When the mass term is not neglected in Eq. (14), we have instead

$$\hat{\sigma}(\omega) = \frac{ne^2/m^*}{(\omega + i\delta)^2 - \omega_c^2} \begin{pmatrix} i\omega & -\omega_c \\ \omega_c & i\omega \end{pmatrix}, \quad (26)$$

and the absorption (which is proportional to $\Re[\sigma_{xx}(\omega)]$) is at the cyclotron frequency ω_c as it should be from Kohn's theorem²⁸.

C. Dynamical matrix in the GRPA

In this work, we obtain the dynamical matrix from the GRPA. This procedures, which uses the density response function $\chi_{\mathbf{K}, \mathbf{K}'}^{(\rho, \rho)}(\mathbf{k}, \omega + i\delta)$ found microscopically to obtain the dynamical matrix for the elastic theory, was developed to study pinned quantum Hall stripes, and is described in detail in Ref. 12. Briefly, we use the fact that the density fluctuations are related to the displacement field via the relation

$$\delta n(\mathbf{k} + \mathbf{K}, t) \approx -i\sqrt{N_s} h(\mathbf{k} + \mathbf{K}) (\mathbf{k} + \mathbf{K}) \cdot \mathbf{u}(\mathbf{k}), \quad (27)$$

to obtain the relation

$$\chi_{\mathbf{K}, \mathbf{K}'}^{(\rho, \rho)}(\mathbf{k}, \tau) = \frac{\nu}{M} \frac{h(\mathbf{k} + \mathbf{K}) h(\mathbf{k} + \mathbf{K}')}{F(\mathbf{k} + \mathbf{K}) F(\mathbf{k} + \mathbf{K}')} \sum_{\alpha, \beta} (k_\alpha + K_\alpha) G_{\alpha, \beta}^{(0)}(\mathbf{k}, \tau) (k_\beta + K'_\beta) \quad (28)$$

between the bare displacement Green's function $G_{\alpha\beta}^{(0)}(\mathbf{k}, \omega)$ and the density response function. The density response function in the GRPA depends on the guiding center densities $\langle \rho(\mathbf{K}) \rangle'$ computed in the Hartree-Fock approximation. The components of the matrix $\widehat{G}^{(0)}(\mathbf{k}, \tau)$ (or of $\widehat{D}_{GRPA}(\mathbf{k})$) are obtained from both the poles and the weight of the density response function.

It is interesting to compare the dynamical matrix obtained in the GRPA from that obtained with other approximations used in the literature. If the filling factor ν is not too small, a rapidly convergent expression for the *classical* dynamical matrix of a lattice of rigid objects with form factor $h(\mathbf{r})$ is given by

$$\widehat{D}_{\text{classical}}(\mathbf{k}) = \frac{2\pi n_s e^2}{\kappa} \sum_{\mathbf{K}} \left[\frac{|h(\mathbf{k} + \mathbf{K})|^2}{|\mathbf{k} + \mathbf{K}|} (\mathbf{k} + \mathbf{K})(\mathbf{k} + \mathbf{K}) - \frac{|h(\mathbf{K})|^2}{|\mathbf{K}|} \mathbf{K}\mathbf{K} \right], \quad (29)$$

where $n_s = N_s/S$ is the density of crystal sites. This expression is not suitable, however, for a lattice of point particles (p.p.). In this case, we can use the expression of $\widehat{D}_{p.p.}(\mathbf{k})$ given by Bonsall and Maradudin²⁰ which is valid to order k^2 .

To compare the three expressions for $\widehat{D}(\mathbf{k})$, we consider the parameterization of the dynamical matrix in terms of the Lamé coefficients λ and μ . The deformation energy of the crystal can be expressed in terms of the dynamical matrix as $F = \frac{1}{2} \sum_{\alpha, \beta} \sum_{\mathbf{k}} u_{\alpha}(\mathbf{k}) D_{\alpha, \beta}(\mathbf{k}) u_{\beta}(-\mathbf{k})$. On the other hand, the same energy is written¹⁷ in elastic theory (and for a triangular lattice) as $F = \frac{1}{2} \int d\mathbf{r} [\lambda(e_{k,k})^2 + 2\mu e_{i,j}^2]$, where $e_{\alpha, \beta} = \frac{1}{2} \left(\frac{\partial u_{\alpha}(\mathbf{r})}{\partial r_{\beta}} + \frac{\partial u_{\beta}(\mathbf{r})}{\partial r_{\alpha}} \right)$ is the strain tensor.

The coefficient μ is actually the shear modulus of the lattice while the bulk modulus is given by $B = S \frac{\partial^2 F}{\partial S^2} = \lambda + \mu$. Comparing the two expressions for F , it is easy to see that the dynamical matrix, in the long-wavelength limit, can be written in terms of the Lamé coefficients as

$$D_{\alpha, \beta}(\mathbf{k}) = n_s^{-1} (\lambda + \mu) k_{\alpha} k_{\beta} + n_s^{-1} \mu k^2 \delta_{\alpha, \beta}. \quad (30)$$

The long-range Coulomb force, absent in the elastic theory, is very important for correctly capturing the low-energy physics. Its inclusion leads to an additional term in λ , *i.e.* to

$$\lambda \rightarrow \left(\frac{2\pi n_s^2 e^2}{\kappa} \right) \frac{M^2}{k} + \eta. \quad (31)$$

The long-wavelength dispersion relation of the magnetophonon mode is given (to order k^2) by

$$\omega = \frac{n_s^{-1} \ell^2}{\hbar M} \sqrt{(\lambda + 2\mu) \mu} k^2. \quad (32)$$

It depends mostly on the shear modulus μ and on the long-range Coulomb part of λ . We will show later that the pinning behavior is also mostly determined by these two quantities.

Using Eq. (30), we can obtain μ_{GRPA} from our numerical data for $\widehat{D}_{GRPA}(\mathbf{k})$. The shear modulus $\mu_{\text{classical}}$ can be obtained by making a small wavevector expansion of Eq. (29) taking into account the appropriate form factor $h(\mathbf{q})$ that depends on M and on the Landau level N . To order k^3 , we find that the Lamé coefficients can be written as

$$\lambda_{\text{classical}} = \left(\frac{2\pi n_s^2 e^2}{\kappa} \right) \left(\frac{M^2}{k} + \alpha_0 + \alpha_1 + 2\alpha_2 - \alpha_3 + \frac{\alpha_4}{3} + \beta_0 k \right), \quad (33)$$

$$\mu_{\text{classical}} = \left(\frac{2\pi n_s^2 e^2}{\kappa} \right) \left(\alpha_3 + \frac{\alpha_4}{3} \right). \quad (34)$$

The detailed forms of the coefficients α'_i s and β'_i s are given in Appendix A.

For a triangular lattice of point particles, we have instead²⁰ (to order k^2)

$$\eta_{p.p.} = -n_s (a + 2b), \quad (35)$$

$$\mu_{p.p.} = n_s b, \quad (36)$$

where $a = -1.225323 \frac{M^2 e^2}{\kappa \sqrt{v_c}}$, $b = 0.245065 \frac{M^2 e^2}{\kappa \sqrt{v_c}}$, with $v_c = \frac{\sqrt{3}}{2} a_0^2$ the unit cell area of the bubble crystal with M electrons.

In Figs. 2 and 3 we compare the three different approximations for the shear modulus. As can be seen from Fig. 2, a point lattice is a good approximation in Landau level $N = 0$ (in comparison with the more exact GRPA result) because the shear modulus does not vary much with filling factor. In $N = 2$, however, the form factor must be

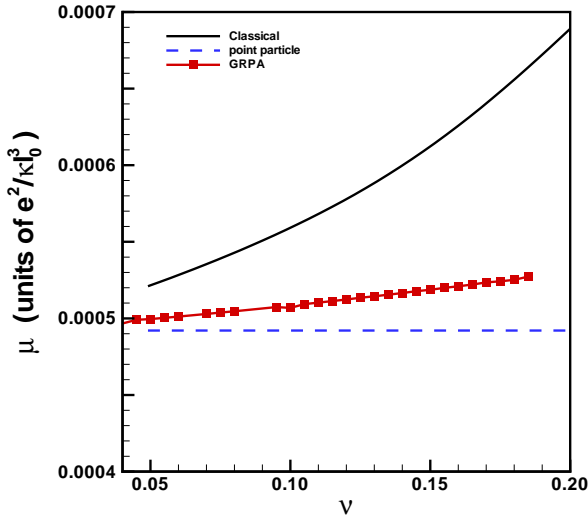


FIG. 2: Shear modulus computed in different approximations for Landau level $N = 0$: for a classical lattice with form factor $h(\mathbf{G})$ (full line); for a lattice of point particle (dashed line) and in the GRPA (line with squares).

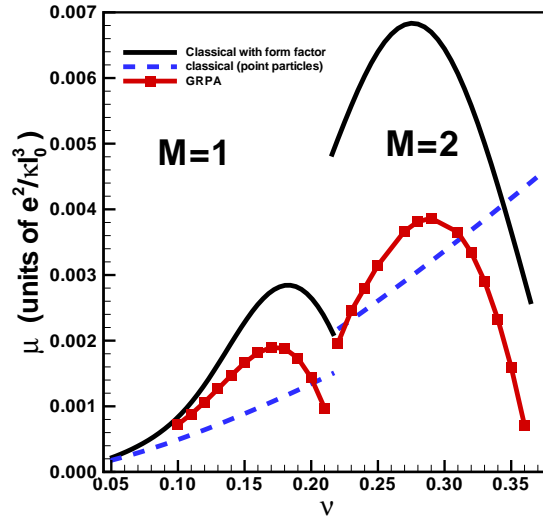


FIG. 3: Shear modulus computed in different approximations for Landau level $N = 2$: for a classical lattice with form factor $h(\mathbf{G})$ (full line); for a lattice of point particle (dashed line) and in the GRPA (line with squares).

considered to account for the softening of the lattice near the transition between two crystal phases. In this case, the GRPA result is qualitatively similar to that of the classical approximation although, quantitatively, the quantum corrections are important especially when considering the jump in the shear modulus at the transition. In the small ν limit, all three approximations give the same result for μ as expected.

Note that in Fig. 3, the shear modulus decreases near ν_2 where the Hartree-Fock calculation predicts a transition to another bubble phase with $M = 3$. In the transport experiments of Lilly et al.²⁴, there is no sign of such transition and, in the rest of this paper, we will refer to the transition region as the region around filling factor ν_1 . The range of filling factor where the $M = 3$ is stable is quite small in the HFA and, in a more accurate calculation, this phase is probably unstable with respect to the stripe phase. Indeed, the $M = 3$ bubble state is absent in DMRG²⁵ calculations.

III. REPLICAS AND THE GAUSSIAN VARIATIONAL METHOD

A. Disorder Coupling

Now we take into account the disorder effect. We assume that the main source of disorder comes from the interface roughness and that it can be represented by a spatially uncorrelated Gaussian random potential $V(\mathbf{r})$. The disorder action reads

$$S_{\text{imp}} = \int d\mathbf{r} \int_0^{1/T} d\tau V(\mathbf{r}) n(\mathbf{r}, \tau), \quad (37)$$

where $V(\mathbf{r})$ has a Gaussian distribution function which leads to the correlator

$$\overline{V(\mathbf{r}_1) V(\mathbf{r}_2)} = V_0^2 v_c \delta(\mathbf{r}_1 - \mathbf{r}_2). \quad (38)$$

Here the overline denotes an average over disorder configurations.

The electron density operator $n(\mathbf{r}, \tau)$ in Eq. (37) must be approximated more accurately than was needed in $G^{(0)}$ in order to capture the possibility of pinning by disorder. Following Giamarchi and Le Doussal¹³, under the assumption of small $\nabla \mathbf{u}(\mathbf{r})$ (which is justified for weak disorder) we write for the bubble crystals

$$n(\mathbf{r}, \tau) = n_0 - n_0 \nabla \cdot \mathbf{u}(\mathbf{r}, \tau) + n_s \sum_{\mathbf{K} \neq 0} h(\mathbf{K}) e^{i\mathbf{K} \cdot [\mathbf{r} - \mathbf{u}(\mathbf{r}, \tau)]}, \quad (39)$$

where $n_0 = n_s h(0)$ is the average electronic density. Fourier transforming, we get

$$n(\mathbf{q}, \tau) \simeq \left[N_0 \delta_{\mathbf{q}, 0} - i\sqrt{N_s} M \mathbf{q} \cdot \mathbf{u}(\mathbf{k}, \tau) + n_s \sum_{\mathbf{K} \neq 0} h(\mathbf{K}) \int d\mathbf{r} e^{i\mathbf{K} \cdot [\mathbf{r} - \mathbf{u}(\mathbf{r}, \tau)] - i\mathbf{q} \cdot \mathbf{r}} \right], \quad (40)$$

where $\mathbf{q} = \mathbf{k} + \mathbf{K}$. Only the last term in Eq. (40) captures the short wavelength oscillations in the charge density and allows pinning by impurities¹³ so that we will drop the first two terms of this equation when using $n(\mathbf{q}, \tau)$ in the disorder action.

B. Effective Form Factor for the Coupling with Disorder

To simplify the coupling with disorder, it is usual to keep only the summation over the first shell of reciprocal lattice vectors in Eq. (40) (*i.e.* 6 vectors for a triangular lattice) as these give the strongest restoring force for the displacement fields. Using Eqs. (1) and (9), one would then be tempted to use, for the form factor $h(\mathbf{K})$ that enters Eq. (40), the expression

$$h(\mathbf{K}) = \frac{M}{\nu} F_N(\mathbf{K}) \langle \rho(\mathbf{K}) \rangle, \quad (41)$$

where $\langle \rho(\mathbf{K}) \rangle$ is the guiding-center density computed in the Hartree-Fock approximation. This choice, however, underestimates the fluctuations in the potential as an electron wavepacket or a bubble moves across the disorder potential. We can capture this energy scale with an effective form factor, that we call $H(\mathbf{K})$, in the following way. The density in the pure crystal is exactly given by

$$n(\mathbf{r}) = \frac{1}{S} \sum_{\mathbf{K}} n(\mathbf{K}) e^{i\mathbf{K} \cdot \mathbf{r}}. \quad (42)$$

The fluctuation in the disorder energy when a large patch of the crystal is slid uniformly is then

$$\begin{aligned} \langle U^2 \rangle &= \int d\mathbf{r} \int d\mathbf{r}' \delta n(\mathbf{r}) \delta n(\mathbf{r}') \langle \overline{V(\mathbf{r}) V(\mathbf{r}')} \rangle, \\ &= \frac{N_s V_0^2}{S^2} \sum_{\mathbf{K} \neq 0} |n(\mathbf{K})|^2. \end{aligned} \quad (43)$$

Using Eqs. (9), (10), and (1) we find

$$\begin{aligned}\langle U^2 \rangle &= \frac{N_s V_0^2}{S^2} \sum_{\mathbf{K} \neq 0} |h(\mathbf{K})|^2, \\ &= \frac{N_s V_0^2}{S^2} \frac{M^2}{\nu^2} \sum_{\mathbf{K} \neq 0} |F_N(\mathbf{K})|^2 |\langle \rho(\mathbf{K}) \rangle|^2,\end{aligned}\quad (44)$$

where $\langle \rho(\mathbf{K}) \rangle$ is computed in the Hartree-Fock approximation. On the other hand, if we describe the fluctuation in the disorder energy by Eq. (40), keeping only one shell of reciprocal lattice vectors with modulus K_0 , we get for the same energy

$$\langle U^2 \rangle \approx \frac{N_s V_0^2}{S^2} 6 |H(K_0)|^2. \quad (45)$$

We define our form factor, $H(K_0)$, by requiring both expressions to be equal so that

$$|H(K_0)|^2 = \frac{1}{6} \frac{M^2}{\nu^2} \sum_{\mathbf{K} \neq 0} |F_N(\mathbf{K})|^2 |\langle \rho(\mathbf{K}) \rangle|^2. \quad (46)$$

In practice, we keep up to 50 shells of reciprocal lattice vectors in the summation on the right hand side of Eq. (46).

From now on $\sum_{\mathbf{K} \neq 0}$ in the disorder action will mean a summation over the first shell of reciprocal lattice vectors. This simplification allows us to compute the Green's function in the presence of disorder in a relatively straightforward manner while retaining the essential physics of pinning so that our results are qualitatively correct. The major effect of these approximations is to replace the soft cutoff in wavevector that would enter through the form factor with a hard one in the reciprocal lattice sum. With this approximation, the impurity action with which we now work is

$$S_{\text{imp}} = n_s \int d\mathbf{r} d\tau V(\mathbf{r}) |H(K_0)| \sum_{\mathbf{K} \neq 0} e^{i\mathbf{K} \cdot [\mathbf{r} - \mathbf{u}(\mathbf{r}, \tau)]}. \quad (47a)$$

C. Replicas and the GVM

A detailed account of the replica and GVM can be found in Ref. 13. In previous work, we generalized this method to study pinning of quantum Hall stripes near half filling in higher Landau levels^{11,12}. Since the formalism can be applied with minor changes to the pinning of the bubble crystals, we refer the reader to these papers for details. In this section we only outline the procedure to obtain the so-called saddle point equations (SPE's).

With the replica trick²¹, one creates n copies of the original action, computes the replicated partition function Z^n , and performs the disorder average on Z^n . Also by taking into account the effective form factor as we discussed before, the resulting effective action is

$$S_{\text{eff}} = S_0^{(\text{eff})} + S_{\text{imp}}^{(\text{eff})}, \quad (48)$$

$$S_0^{(\text{eff})} = \frac{1}{2T} \sum_{a=1}^n \sum_{\mathbf{k}, \omega_n} \sum_{\alpha, \beta=x, y} u_\alpha^a(\mathbf{k}, \omega_n) G_{\alpha\beta}^{(0)-1}(\mathbf{k}, \omega_n) u_\beta^a(-\mathbf{k}, -\omega_n), \quad (49)$$

$$\begin{aligned}S_{\text{imp}}^{(\text{eff})} &\simeq -v_{\text{imp}} \sum_{a, b=1}^n \int_0^{1/T} d\tau_1 \int_0^{1/T} d\tau_2 \sum_{\mathbf{r}} \sum_{\mathbf{K} \neq 0} |H(K_0)|^2 \\ &\times \cos [\mathbf{K} \cdot [\mathbf{u}^a(\mathbf{r}, \tau_1) - \mathbf{u}^b(\mathbf{r}, \tau_2)]],\end{aligned} \quad (50)$$

where $v_{\text{imp}} = V_0^2 v_c^2 n_s^2$, and a, b are replica indices that run from 1 to n . In obtaining the last line of Eq. (50) we have neglected some rapidly oscillating terms.

In the pure limit, the action is diagonal in the replica indices. Disorder averaging introduces a coupling among the replicas through the impurity coupling $S_{\text{imp}}^{(\text{eff})}$ in Eq. (50). This coupling is non-Gaussian so we next apply the GVM to get a simplified expression. The fundamental idea of the GVM is to replace S_{eff} with a variational action S_{var} that is *quadratic*. We write

$$S_{\text{var}} = \frac{1}{2T} \sum_{\mathbf{k}, \omega_n} u_\alpha^a(\mathbf{k}, \omega_n) (G^{-1})_{\alpha\beta}^{ab}(\mathbf{k}, \omega_n) u_\beta^b(-\mathbf{k}, -\omega_n), \quad (51)$$

with the coefficients $(G^{-1})_{\alpha\beta}^{ab}(\mathbf{k}, \omega_n)$ chosen to best match the original problem. This is accomplished by minimizing a free energy¹³ $F_{\text{var}} = F_0 + T [\langle S \rangle_{S_{\text{var}}} - \langle S_{\text{var}} \rangle_{S_{\text{var}}}]$ where F_0 is the free energy associated with the action S_{var} , and $\langle \dots \rangle_{S_{\text{var}}}$ indicates a functional integral over displacements, with S_{var} as a weighting function. In Eq. (51), $G_{\alpha\beta}^{ab}(\mathbf{k}, \omega_n)$ is the displacement Green's function,

$$G_{\alpha\beta}^{ab}(\mathbf{k}, \omega_n) = \int_0^{1/T} d\tau \langle T_\tau u_\alpha^a(\mathbf{k}, \tau) u_\beta^b(-\mathbf{k}, 0) \rangle_{S_{\text{var}}}. \quad (52)$$

It is convenient to write it in terms of the bare Green's function via the equation

$$(G^{-1})_{\alpha\beta}^{ab}(\mathbf{k}, \omega_n) = G_{\alpha\beta}^{(0)-1}(\mathbf{k}, \omega_n) \delta_{ab} - \zeta_{\alpha\beta}^{ab}(\omega_n), \quad (53)$$

where $\zeta_{\alpha\beta}^{ab}(\omega_n)$ is the element of the variational self-energy matrix $\hat{\zeta}$. Note that there is no \mathbf{k} dependence in $\hat{\zeta}$ because we have chosen our impurity action to be local in space; this will become clear when we find the SPE's below. Note also the obvious symmetries $G^{ab} = G^{ba}$ and $\zeta^{ab} = \zeta^{ba}$.

D. Saddle Point Equations (SPE's)

Finding the extremum of the free energy leads to the saddle point equations (SPE's)

$$\zeta_{\alpha\beta}^{aa}(\omega_n) = 4v_{\text{imp}} \int_0^{1/T} d\tau \left\{ (1 - \cos \omega_n \tau) V'_{\alpha\beta} [B^{aa}(\tau)] + \sum_{b \neq a} V'_{\alpha\beta} [B^{ab}(\tau)] \right\}, \quad (54)$$

$$\zeta_{\alpha\beta}^{a(b \neq a)}(\omega_n) = -4v_{\text{imp}} \int_0^{1/T} d\tau \cos \omega_n \tau V'_{\alpha\beta} [B^{ab}(\tau)], \quad (55)$$

where

$$V'_{\alpha\beta} [B^{ab}(\tau)] = \sum_{\mathbf{K} \neq 0} |H(K_0)|^2 K_\alpha K_\beta \exp \left[-\frac{1}{2} \sum_{\mu\nu=x,y} K_\mu K_\nu B_{\mu\nu}^{ab}(\tau) \right], \quad (56)$$

and

$$\begin{aligned} B_{\alpha\beta}^{ab}(\tau) &= \langle T_\tau [u_\alpha^a(\mathbf{r}, \tau) - u_\beta^b(\mathbf{r}, 0)]^2 \rangle_{S_{\text{var}}} \\ &= T \frac{1}{N_s} \sum_{\mathbf{k}, \omega_n} [G_{\alpha\beta}^{aa}(\mathbf{k}, \omega_n) + G_{\alpha\beta}^{bb}(\mathbf{k}, \omega_n) - 2 \cos(\omega_n \tau) G_{\alpha\beta}^{ab}(\mathbf{k}, \omega_n)]. \end{aligned} \quad (57)$$

It is apparent at this point that the self-energy has no \mathbf{k} dependence. Moreover, if we assume that reflection symmetry for the bubble crystals are not spontaneously broken after disorder averaging, then the solutions of interest to Eqs. (54) and (55) will satisfy $\zeta_{xy}^{ab} = 0$ and $\zeta_{xx}^{ab} = \zeta_{yy}^{ab}$. Using the symmetry [see Eq. (30)] of the dynamical matrix $D_{xx}(k_x, k_y) = D_{yy}(k_y, k_x)$ for a triangular lattice, we can also show that $\zeta_{xx}^{ab} = \zeta_{yy}^{ab}$ is a solution of the SPE's. We need thus solve for one self-energy component only.

At this point, we take the limit $n \rightarrow 0$ in the replica index. In taking this limit, one *assumes* that the self-energy and Green's function matrices can be written in a “hierarchical form”²¹. A consequence of this is that the replica index becomes a continuous variable $u \in [0, 1]$ (The variable u must not be confused with the displacement field here.) For example, the self-energy matrix is now characterized by a diagonal component, ζ_α , and an off-diagonal component, $\zeta_\alpha(u)$, such that

$$\zeta_{\alpha\alpha}^{aa} \rightarrow \zeta_\alpha, \quad (58)$$

$$\zeta_{\alpha\alpha}^{ab(\neq a)} \rightarrow \zeta_\alpha(u), \quad \text{for } 0 \leq u \leq 1. \quad (59)$$

Similarly, $G_{\alpha\beta}^{aa} \rightarrow \tilde{G}_{\alpha\beta}$, $G_{\alpha\beta}^{ab(\neq a)} \rightarrow G_{\alpha\beta}(u)$ ($0 \leq u \leq 1$). Since the disorder potential $V(\mathbf{r})$ is time independent, a further simplification one finds is that the off-diagonal replica components $\zeta_{\alpha\alpha}^{ab(\neq a)}$ and $G_{\alpha\beta}^{ab(\neq a)}$ are τ independent¹³ so that $\hat{G}(\mathbf{k}, \omega_n, u)$ and $\hat{\zeta}(\mathbf{k}, \omega_n, u)$ are different from zero only for $\omega_n = 0$. We have

$$\hat{G}(\mathbf{k}, \omega_n, u) = \hat{G}(\mathbf{k}, u) \delta_{\omega_n, 0}, \quad (60)$$

$$\hat{\zeta}(\omega_n, u) = \hat{\zeta}(u) \delta_{\omega_n, 0}. \quad (61)$$

The SPE's (54) and (55) for the *diagonal component* $\tilde{\zeta}_{xx} = \tilde{\zeta}_{yy} \equiv \tilde{\zeta}$ may now be written as

$$\tilde{\zeta}(\omega_n) = \int_0^1 du \zeta(u) + 4v_{\text{imp}} \int_0^{1/T} d\tau (1 - \cos(\omega_n \tau)) V'_{xx} [\tilde{B}(\tau)], \quad (62)$$

$$\zeta(u) = -\frac{4v_{\text{imp}}}{T} V'_{xx} [B(u)], \quad (63)$$

where, from Eq. (57),

$$\tilde{B}_{xx}(\tau) = 2T \sum_{\mathbf{k}, \omega_n} (1 - \cos(\omega_n \tau)) \tilde{G}_{xx}(\mathbf{k}, \omega_n), \quad (64)$$

$$B_{xx}(u) = 2T \sum_{\mathbf{k}} \left\{ \left[\sum_{\omega_n} \tilde{G}_{xx}(\mathbf{k}, \omega_n) \right] - G_{xx}(\mathbf{k}, u) \right\}. \quad (65)$$

Note that Eq. (62) also gives us $\tilde{\zeta}(\omega_n = 0) = \int_0^1 du \zeta(u)$.

To compute the dynamical conductivities in Eq. (24), we first need to solve the SPE's for the finite-frequency self energy $\tilde{\zeta}(\omega_n)$. If we take the analytical continuation of Eq. (62), we get

$$\begin{aligned} \tilde{\zeta}^{\text{ret}}(\omega) &= e_0 - 24v_{\text{imp}} |H(K_0)|^2 K_0^2 \int_0^\infty dt (e^{i\omega t} - 1) \\ &\times \text{Im} \exp \left\{ -\frac{K_0^2}{\pi} \int_0^\infty df \text{Im} \left[\sum_{\mathbf{k}} \tilde{G}_{xx}^{\text{ret}}(\mathbf{k}, \omega) \right] (1 - e^{-ift}) \right\} \end{aligned} \quad (66)$$

where $e_0 = \tilde{\zeta}^{\text{ret}}(0^+)$ is a constant which will be determined below. Eqs. (60) and (61) indicate that for non-zero frequency ω_n ,

$$\tilde{G}_{xx}(\mathbf{k}, \omega_n \neq 0) = \left[\tilde{G}^{(0)-1}(\mathbf{k}, \omega_n) - \hat{\tilde{\zeta}}(\omega_n) \right]_{xx}^{-1}. \quad (67)$$

Thus, once we have obtained the self-energy, we can easily compute the finite-frequency conductivities in Eq. (24) by analytically continuing Eq. (67) to real frequency. The retarded Green's function for the displacement field is given by

$$\tilde{G}_{xx}^{\text{ret}}(\mathbf{k}, \omega \neq 0) = \left[\tilde{G}_{\text{ret}}^{(0)-1}(\mathbf{k}, \omega) - \hat{\tilde{\zeta}}^{\text{ret}}(\omega) \right]_{xx}^{-1}, \quad (68)$$

and so

$$G(\mathbf{k}, \omega) = \frac{\begin{pmatrix} D_{yy}(\mathbf{k}) - \tilde{\zeta}^{\text{ret}}(\omega) & \frac{-i\omega M}{\ell^2} - D_{xy}(\mathbf{k}) \\ \frac{i\omega M}{\ell^2} - D_{yx}(\mathbf{k}) & D_{xx}(\mathbf{k}) - \tilde{\zeta}^{\text{ret}}(\omega) \end{pmatrix}}{\det[D] - \tilde{\zeta}^{\text{ret}}(\omega) \text{tr}[D] + \left(\tilde{\zeta}^{\text{ret}}(\omega_n) \right)^2 - M^2 \omega^2 / \ell^4}. \quad (69)$$

Inserting this result into Eq. (24), we obtain our final expression for the longitudinal conductivity in the presence of disorder,

$$\sigma_{xx}(\omega) = \sigma_{yy}(\omega) = \frac{M^2 e^2}{v_c} \frac{i\omega \tilde{\zeta}^{\text{ret}}(\omega)}{\left[\tilde{\zeta}^{\text{ret}}(\omega) \right]^2 - M^2 \omega^2 / \ell^4}. \quad (70)$$

E. Semiclassical approximation

Equation (66) for the self-energy is a very complex self-consistent equation. In studying the stripe phase^{11,12}, where a depinning transition may take place and relative fluctuations in the displacement field can become very large, we found out that it was necessary to solve this equation exactly. In the case of the bubble crystals, the transition between the bubble phases are first order and we expect that the fluctuations in the relative displacement of the

bubbles are small enough so that we can use a semiclassical version of Eq. (66). The semiclassical expression for the self-energy¹³ is obtained by expanding the exponential in Eq. (56) and keeping only the leading term. This leads to

$$\tilde{\zeta}^{\text{ret}}(\omega) = e_0 + \frac{\Delta}{N_s} \sum_{\mathbf{k}} \left[\tilde{G}_{xx}^{\text{ret}}(\mathbf{k}, \omega) - \tilde{G}_{xx}^{\text{ret}}(\mathbf{k}, \omega = 0^+) \right], \quad (71)$$

where

$$\Delta = 12v_{\text{imp}} |H(K_0)|^2 K_0^4. \quad (72)$$

The semiclassical approximation is a powerful simplification when it is valid. In particular one sees that Eq. (71) is local in the frequency ω so that $\tilde{\zeta}^{\text{ret}}(\omega)$ can be determined one frequency at a time. As we will see later, $e_0 \neq 0$ is an energy offset that, in a pinned state, opens a gap in the phonon spectrum.

F. A Constraint for e_0

The SPE (71) becomes a set of two coupled equations for the real and imaginary parts of the self-energy if e_0 is known. Formally, e_0 needs to be determined self-consistently by solving Eq. (71) together with those for $\zeta(u)$. The SPE's have a family of solutions parameterized by u_c where u_c is, in principle, determined by minimizing the free energy. In the case of spatial dimension $d > 2$, u_c determined in this way leads to $\Re[\sigma_{\alpha\alpha}(\omega)] \sim \omega^2$ at small ω . This behavior is consistent with arguments by Mott as well as with some exact solutions²² (up to a logarithmic correction). For $d \leq 2$, however, this way of finding u_c can yield an unphysical result in which, in the pinned state, the conductivity shows a true gap *i.e.* $\Re[\sigma(\omega)]$ vanishes below some finite frequency. For $d \leq 2$, what can instead be done is to *impose* the condition $\Re[\sigma_{\alpha\alpha}(\omega)] \sim \omega^2$ at small ω . This common procedure, although not fully understood, leads to physically reasonable results and we will adopt it in the computations that follow. (The reader should keep in mind that it leads to a broader response in the WC regime than is found by other methods. We discuss this issue below.) From Eq. (70), this condition is equivalent to the condition $\Im[\tilde{\zeta}^{\text{ret}}(\omega)] \sim \omega$ at small ω and this guarantees that the magnetophonon mode density of states vanishes at zero frequency as it should for a pinned system.

To determine e_0 , we thus write, for small ω ,

$$\tilde{\zeta}_{\text{ret}}(\omega) \approx e_0 + i\beta\omega. \quad (73)$$

With this constraint in Eq. (71), using Eq. (69) and the symmetry relation $\tilde{\zeta}_{xx}^{\text{ret}}(\omega) = \tilde{\zeta}_{yy}^{\text{ret}}(\omega)$, we can easily show that the condition for nonvanishing β leads to

$$1 = -\Delta \sum_{\mathbf{k}} \left[\frac{\det[D] + e_0 \text{tr}[D] - e_0^2 - \frac{1}{2}(\text{tr}[D])^2}{(\det[D] - e_0 \text{tr}[D] + e_0^2)^2} \right]. \quad (74)$$

Eq. (74) is the constraint which we solve numerically to get e_0 .

IV. NUMERICAL RESULTS

We now discuss our numerical results for the behavior of the dynamical conductivity $\sigma_{xx}(\omega)$ with filling factor in Landau level $N = 2$. Figures 4 and 5 show the real part of the dynamical conductivity $\Re[\sigma_{xx}(\omega)]$ for different values of the filling factor ν in the $M = 1$ and $M = 2$ bubble phases. At the transition between two bubble phases, the density is such that the cyclotron radius $R_c = \sqrt{2N+1}\ell$ of adjacent bubbles touches one another. Away from the transition region, however, the size of the bubbles is smaller than the lattice spacing. For all filling factors here we assume the bubbles are much bigger than the correlation length of the disorder (which we take as zero).

We plot in Fig. 6 (a) the peak (or pinning) frequency $f_{pk} = 2\pi\omega_{pk}$, (b) the full width at half maximum of the resonance, Δf_{pk} , and (c) the quality factor $Q = f_{pk}/\Delta f_{pk}$. Although we do not expect our theory to be quantitatively accurate, we choose the disorder level in our calculation so that our pinning frequency at $\nu = 0.1$ is equal to that measured experimentally⁷ at the same filling factor; *i.e.*, $f_{pk} \approx 1.5$ GHz with an electronic density of $n = 3.0 \times 10^{11}$ cm⁻². We find that our results are in a very good qualitative agreement with those of Lewis et al.⁷ with the exception of the region between $\nu_a = 0.16$ to $\nu_b = 0.28$ where the two phases are assumed to coexist.

The variation of the conductivity with ν is the same for the $M = 1$ and $M = 2$ phases. In both cases the conductivity curve has a non-Lorentzian lineshape with a peak frequency and width that decrease with increasing filling factor ν (or

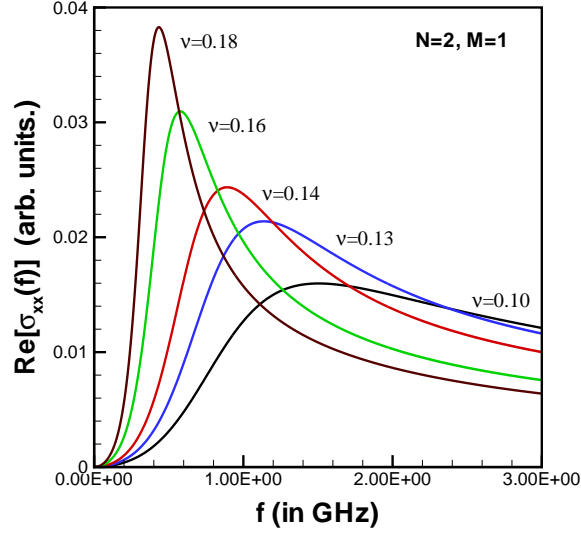


FIG. 4: Dynamical conductivity for the Wigner crystal in Landau level $N = 2$.

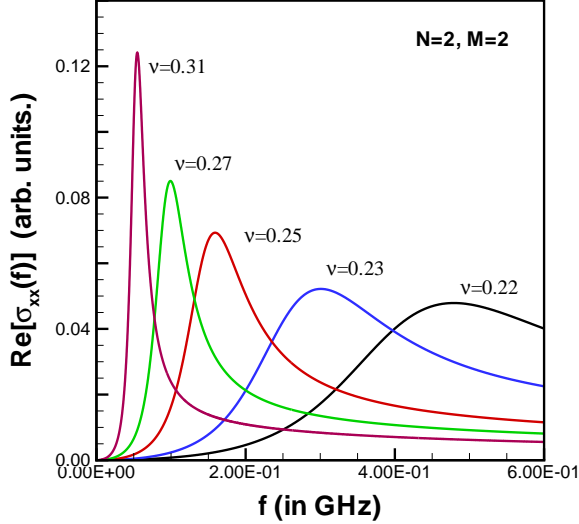


FIG. 5: Dynamical conductivity for the $M = 2$ bubble crystal in Landau level $N = 2$.

density) and a peak height that increases with increasing filling factor. This behavior is qualitatively consistent with that of a weak-pinning model. Quantitatively, however, our pinning frequency decreases faster (we find $f_{pk} \sim 1/\nu^3$, for $M = 1$) than what is seen experimentally where the dependence $f_{pk} \sim 1/\nu^{3/2}$ is found. The width of the pinning peak and the quality factor that we get, however, are typical of what are measured experimentally.

If we compare the behavior of the pinning frequency in Fig. 6 with that of the shear modulus calculated in Fig. 3, we see that the pinning frequency behavior is opposite to that of the shear modulus within the whole range of filling factor considered. A more rigid crystal is less sensitive to the disorder potential and has, as a consequence, a smaller pinning frequency. This is precisely what is expected from collective pinning theory²⁷.

The increase in the pinning frequency that we get after $\nu \approx 0.18$ in the $M = 1$ phase is not seen experimentally. Instead, two pinning frequencies separated by a gap of the order of 0.2 GHz are detected in the region between the dashed lines in Fig. 1. These two frequencies are found to be nearly frequency independent in this range (*i.e.*

from $\nu_a = 0.16$ to $\nu_b = 0.28$) where the two crystal phases probably coexist. Interestingly, the difference in pinning frequencies at the endpoints of this interval, $f_{pk}(\nu_a) - f_{pk}(\nu_b)$, is 0.42 GHz in our calculation. We remark that the choice of the form factor $H(\mathbf{K}_0)$ [see Eq. (46)] that enters in the coupling with the disorder [Eq. (50)] is important in getting the right order of magnitude for the drop in the pinning frequency. We find, for example, that replacing the $\sum'_{\mathbf{K} \neq 0} |H(K_0)|^2 (\dots)$ in Eq. (50) (the sum is here on the first shell of reciprocal lattice vectors only) by the more naïve form $\sum_{\mathbf{K} \neq 0} |h(\mathbf{K})|^2 (\dots)$ (where the sum is over all reciprocal lattice vectors) and using a cutoff in \mathbf{K} in this last expression overestimate the sudden reduction in the pinning frequency seen experimentally⁷. The formalism we use needs to be generalized in order for us to properly compute the dynamical conductivity in the coexistence region.

In Landau level $N = 0$, our numerical calculations give results similar to those of Chitra and coworkers.¹⁴ For uncorrelated disorder, the pinning frequency increases continuously with decreasing filling factor (at fixed density). For a disorder level (v_{imp} in our calculation) corresponding to the typical peak frequencies observed experimentally³, we get a quality factor Q of the order of 1. We have found that if one solves the GVM equations for *very* small disorder values in Landau level $N = 0$, a sharp resonance emerges with $Q \sim \Delta^{-1/4}$. However, this behavior appears only at disorder strengths yielding resonance frequencies far below those observed in experiment.

We note that experiments on higher density *hole* systems^{30,31} have revealed dramatically narrower resonances, a phenomenon that our present calculations do not seem to reproduce. We discuss this issue in the next section.

V. LONG RANGE COULOMB INTERACTION AND WIDTH OF THE PINNING PEAK

One issue regarding the lineshape of the dynamical conductivity near the pinning frequency involves the observation in hole systems, in the Wigner crystal regime, of pinning peaks with quality factor Q of order 5 and even higher^{30,31}.

The possibility of such dramatic narrowing was suggested by one of us¹⁵ as being a result of the long-range Coulomb interaction, in conjunction with the effect of the magnetic field. In Ref. 15, a simulation of an electron system in a strong magnetic field with a simplified disorder model yielded a *remarkably* sharp resonance, with width so narrow it could not be determined numerically. That this effect was related to the long-range nature of the Coulomb interaction was demonstrated by running the same simulation with a screened interaction, which yielded a more typical pinning peak with $Q \sim 1$.

How such a narrow resonance might be attained can be understood in a self-consistent Born approximation (SCBA). Writing the self-energy as $\zeta(\omega) = z_1 + iz_2$, the imaginary part $z_2(\omega)$ at the resonance frequency sets the width of the pinning peak. The SCBA can be written in the form

$$\zeta(\omega) = \Delta \int d^2q G_{xx}^{ret}(\mathbf{q}, \omega), \quad (75)$$

where Δ is the scale of the disorder interaction defined in Eq. (72). The similarity of this equation with the semiclassical approximation in the GVM [Eq. (71)] is apparent, and indeed if one takes the imaginary part of Eq. (75) it is identical to the imaginary part of Eq. (71). This equation can be written explicitly in the form

$$1 = \Delta \int d^2q \frac{\frac{1}{2}(tr[D])^2 - \det[D] + \omega^2 - z_1 tr[D] + z_1^2 + z_2^2}{[\det[D] + z_1^2 - z_2^2 - \omega^2 - z_1 tr[D]]^2 + z_2^2 [tr[D] - 2z_1]^2}. \quad (76)$$

A solution to Eq. (76) appears at first challenging for small Δ because the right hand side appears to vanish as $\Delta \rightarrow 0$ whereas the left hand side remains at one. A solution is always possible for any given value of z_1 because the integral is logarithmically divergent as $z_2 \rightarrow 0$. This can be seen by noting that at small q , the trace and determinant respectively have the forms $tr[D(\mathbf{q})] = Yq$ and $\det[D(\mathbf{q})] = \alpha q^3$. (Note for short range interactions the powers of q in each of these expressions increase by 1.) If we choose $\omega = -z_1(\omega)$, *i.e.*, the resonance frequency, the small frequency limit of the integrand gives

$$1 \approx 4\pi\Delta \int_0^{q_c} dq \frac{q}{Y^2 q^2 + 4z_2^2}, \quad (77)$$

with $q_c = \sqrt{z_1 Y / \alpha}$. We then arrive at a solution of the form

$$z_2 \approx \frac{Y q_c}{2} e^{-Y^2 / 4\pi\Delta}. \quad (78)$$

A very similar result was obtained in Ref. 15 using a different method. The exponential behavior in Eq. (78) allows for a very narrow resonance, as was found in the simulation. As discussed in Ref. 15, the result may be understood

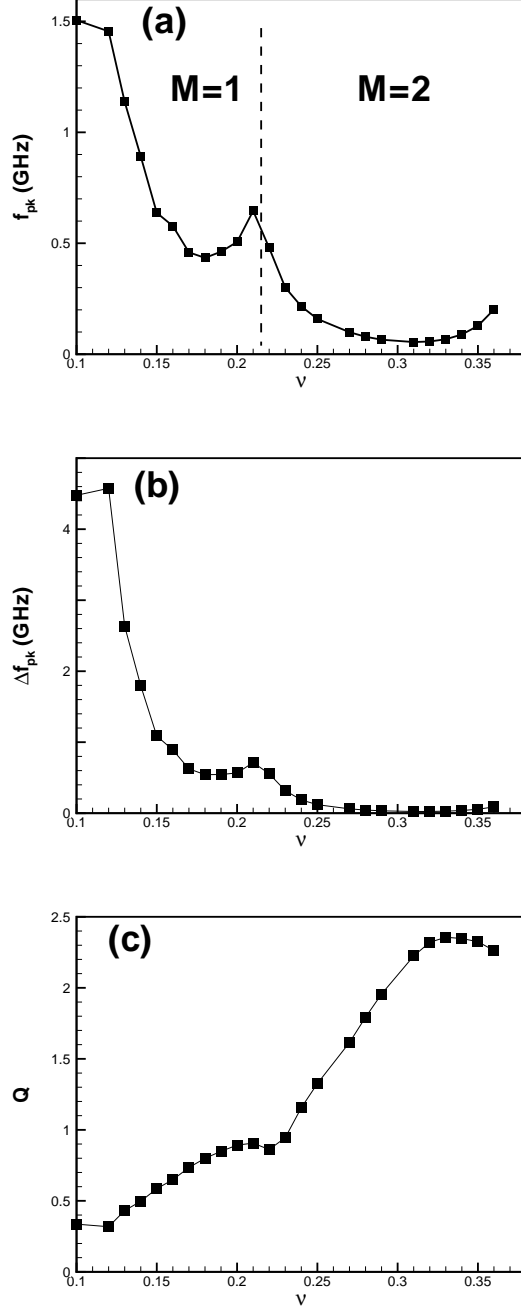


FIG. 6: Numerical results for the bubble phases in Landau level $N = 2$ for (a) the pinning peak; (b) the width of the pinning peak; (c) the quality factor.

as being due to a suppression of the collective mode density of states at low frequencies, arising from the effectively very large stiffness that is a result of the Coulomb interaction.

Given the similarity between Eqs. (76) and (71), it is surprising that the GVM approach does not obtain this narrow resonance. The reason for this difference can be understood by the way in which the GVM is *different* from the SCBA, specifically by how e_0 is determined. By definition, $e_0 = z_1(\omega \rightarrow 0)$, which is obtained in the SCBA by self-consistently solving the real part of Eq. (75). A major limitation of this approach is that it does not correctly capture under most circumstances the competition between elasticity and pinning energy that sets the pinning frequency^{26,27}. In the GVM, e_0 is obtained by solving Eq. (74), which followed from requiring $\Re[\sigma_{\alpha\alpha}(\omega)] \sim \omega^2$ at small ω . There is

a very close connection between Eqs. (74) and (77): the integrands are *identical* for $q/q_c \gg 1$. Because q_c becomes very small for small disorder, by noting that $z_1(\omega)$ is not very different than e_0 near the resonance we can see the choice of e_0 *guarantees* that Eq. (76) will very nearly be satisfied from the portion of the integral where $|\mathbf{q}| \geq q_c$. The small differences in the two equations can then be accommodated with a value of z_2 not very different than z_1 . This leads to the more typical result for a pinned system, $Q \sim 1$.

We conclude this section with a few comments. First, it should be noted that the very sharp resonances predicted by the SCBA and related work^{15,16} are *not* what is observed experimentally. While the hole experiments yield peaks with a surprisingly large Q , they are many orders of magnitude smaller than what is predicted by Eq. (78). If such a very narrow resonance is the correct expectation for the pinned Coulomb system, then there is presumably some dissipation mechanism that has not been identified. One cannot help but notice, however, that the results of replicas+GVM method are far more similar to the experimental results than the SCBA by itself gives. And while the simulation reported in Ref. 15 suggests a very narrow resonance, it is possible that the simplified disorder model used there may give a different result than a generic disorder model (although previous studies have suggested this should not be the case³²).

Secondly, it should be emphasized that the choice of e_0 in Eq. (74) really is very special. If e_0 is allowed to vary even by a very small amount from the solution of this equation, we have verified that the semiclassical approximation to the SPE's [Eq. (71)] results in a very sharp resonance as expected from the SCBA. This demonstrates that the important difference between the method used in this paper and the SCBA is not really in the use of replicas or the GVM, but rather the introduction of the extra constraint. Indeed, it was suggested by Fogler and Huse¹⁶ that if one can instead impose a condition $\Re[\sigma_{\alpha\alpha}(\omega)] \sim \omega^x$ with a large value of x , then the Q of the resulting resonance is again extremely large – smaller than what is expected from the SCBA, but still orders of magnitude larger than what is seen in experiment.

A third important point is that, although these considerations leave us with questions about the Q of the resonance, it seems likely the resonance frequency itself is well-represented by the calculations described in this work. This is because the pinning resonance is determined by collective pinning, which balances the lowest two energy scales – elastic and disorder interactions – to determine the restoring force for motion of the system as a whole. (Again, we emphasize that even a very small adjustment of e_0 results in a narrow resonance. The resonance frequency does not need to change noticeably to dramatically increase Q .) A resonance frequency determined by collective pinning is consistent with what was found in the simulation of Ref. 15.

As we have seen, the GVM+replicas method, together with the e_0 constraint, yields results that generally compare favorably with experiment. Other methods such as the SCBA yield much sharper resonances than are observed. Nevertheless, it is possible that such sharp resonances are the correct response for the model we are analyzing, in which case the mechanism that leads to pinning peaks with $Q \sim 1$ in experiment remains unknown. We leave these questions for future research.

VI. CONCLUSION

We have studied the behavior of the pinning peak of the Wigner and bubble crystals in Landau level $N = 2$ as a function of the filling factor. We used an elastic action obtained from the Hartree-Fock and time-dependent Hartree-Fock approximations and treated the disorder averaging using the replica trick and Gaussian Variational Method. Comparisons with recent microwave experiments in $N = 2$ show that the predictions of our model for the dependence of the pinning frequency and width of the pinning peak with filling factor compare favorably with experiment. At the moment, however, our approach can not reproduce the pinning frequencies observed in some range of filling factor in $N = 2$ where the Wigner crystal and the $M = 2$ bubble phases are believed to coexist. Finally, we discussed the relation of this method with those that predict a very narrow resonance.

VII. ACKNOWLEDGEMENTS

The authors want to thank R. Lewis, L. Engel and Y. Chen and C. Doiron for several useful discussions. This work was supported by a research grant (for R.C.) and undergraduate research grants (for A.F.) both from the Natural Sciences and Engineering Research Council of Canada (NSERC) and by a research grant from the Fonds Québécois pour la recherche sur la nature et les technologies (FQRNT). H.A.F. acknowledges the support of NSF through Grant No. DMR-0454699.

APPENDIX A: LONG WAVELENGTH EXPANSION OF THE DYNAMICAL MATRIX

The dynamical matrix is given by Eq. (29) *i.e.*

$$\overleftrightarrow{D}(\mathbf{k}) = \frac{2\pi n_s e^2}{\kappa} \sum_{\mathbf{K}} \left[\Upsilon(\mathbf{k} + \mathbf{K}) |\Lambda(\mathbf{k} + \mathbf{K})|^2 (\mathbf{k} + \mathbf{K})(\mathbf{k} + \mathbf{K}) - \Upsilon(\mathbf{K}) |\Lambda(\mathbf{K})|^2 \mathbf{K} \mathbf{K} \right], \quad (\text{A1})$$

where

$$\Lambda(\mathbf{k}) \equiv h^2(\mathbf{k}), \quad (\text{A2})$$

$$\Upsilon(\mathbf{k}) \equiv \frac{1}{|\mathbf{k} + \mathbf{K}|}. \quad (\text{A3})$$

We want to find an expression for the dynamical matrix in the long-wavelength limit valid up to order k^3 . For the form factor, we use Eqs. (10),(11). We expand the interaction and the form factors to order k^3 and define in this way the coefficients $\Upsilon_0, \Upsilon_1, \Upsilon_2, \Upsilon_3$ and $\Lambda_0, \Lambda_1, \Lambda_2, \Lambda_3$:

$$\Upsilon(|\mathbf{k} + \mathbf{K}|) \approx \Upsilon_0(K) + \Upsilon_1(K)(\mathbf{k} \cdot \mathbf{K}) + \Upsilon_2(K)k^2 + \Upsilon_3(K)(\mathbf{k} \cdot \mathbf{K})^2, \quad (\text{A4})$$

$$\Lambda(|\mathbf{k} + \mathbf{K}|) \approx \Lambda_0(K) + \Lambda_1(K)(\mathbf{k} \cdot \mathbf{K}) + \Lambda_2(K)k^2 + \Lambda_3(K)(\mathbf{k} \cdot \mathbf{K})^2. \quad (\text{A5})$$

In these expressions, all coefficients depend only on the modulus of \mathbf{K} . For $\mathbf{K} = 0$, we need the expansion to order k^2 of the form factor so that we define the coefficients λ_1 and λ_2 by

$$\Lambda(\mathbf{k}) = M^2 + \lambda_1 k + \lambda_2 k^2. \quad (\text{A6})$$

The coefficients λ_1, λ_2 and $\Lambda_0, \Lambda_1, \Lambda_2, \Lambda_3$ depends on the particular form factor that is choosen while $\Upsilon_0(K) = \frac{1}{K}$, $\Upsilon_1(K) = -\frac{1}{K^3}$, $\Upsilon_2(K) = -\frac{1}{2K^5}$, and $\Upsilon_3(K) = \frac{3}{2K^5}$.

Using the inversion and reflexion symmetries of the triangular lattice, we find, after some algebra, that

$$D_{xx}(\mathbf{k}) = \left(\frac{2\pi n_s e^2}{\kappa} \right) \left[\left(\frac{M^2}{k} + \alpha_0 + \alpha_1 + 2\alpha_2 + \alpha_3 + \alpha_4 + \beta_0 k \right) k_x^2 + \left(\alpha_3 + \frac{\alpha_4}{3} \right) k_y^2 \right], \quad (\text{A7})$$

$$D_{yy}(\mathbf{k}) = \left(\frac{2\pi n_s e^2}{\kappa} \right) \left[\left(\frac{M^2}{k} + \alpha_0 + \alpha_1 + 2\alpha_2 + \alpha_3 + \alpha_4 + \beta_0 k \right) k_y^2 + \left(\alpha_3 + \frac{\alpha_4}{3} \right) k_x^2 \right], \quad (\text{A8})$$

$$D_{xy}(\mathbf{k}) = \left(\frac{2\pi n_s e^2}{\kappa} \right) \left(\frac{M^2}{k} + \alpha_0 + \alpha_1 + 2\alpha_2 + \frac{2\alpha_4}{3} + \beta_0 k \right) k_x k_y = D_{yx}(\mathbf{k}), \quad (\text{A9})$$

where we have defined $\alpha_0 = \lambda_1$, $\beta_0 = \lambda_2$, and

$$\alpha_1 = \sum_{\mathbf{K} \neq 0} \Lambda_0(K) \Upsilon(K), \quad (\text{A10})$$

$$\alpha_2 = \sum_{\mathbf{K} \neq 0} [\Upsilon_0(K) \Lambda_1(K) + \Upsilon_1(K) \Lambda_0(K)] K_x^2, \quad (\text{A11})$$

$$\alpha_3 = \sum_{\mathbf{K} \neq 0} [\Lambda_0(K) \Upsilon_2(K) + \Lambda_2(K) \Upsilon_0(K)] K_x^2, \quad (\text{A12})$$

$$\alpha_4 = \sum_{\mathbf{K} \neq 0} [\Lambda_0(K) \Upsilon_3(K) + \Lambda_1(K) \Upsilon_1(K) + \Lambda_3(K) \Upsilon_0(K)] K_x^4. \quad (\text{A13})$$

With the dynamical matrix written as

$$D_{\alpha,\beta}(\mathbf{k}) = n_s^{-1} (\lambda + \mu) k_\alpha k_\beta + n_s^{-1} \mu k^2 \delta_{\alpha,\beta}, \quad (\text{A14})$$

the Lamé coefficients are thus given by

$$\lambda = \left(\frac{2\pi n_s^2 e^2}{\kappa} \right) \left(\frac{M^2}{k} + \alpha_0 + \alpha_1 + 2\alpha_2 - \alpha_3 + \frac{\alpha_4}{3} + \beta_0 k \right), \quad (\text{A15})$$

$$\mu = \left(\frac{2\pi n_s^2 e^2}{\kappa} \right) \left(\alpha_3 + \frac{\alpha_4}{3} \right). \quad (\text{A16})$$

The correction $\beta_0 k$ to the Lamé coefficient λ (and so to the bulk modulus) comes from the $\mathbf{K} = 0$ term in the summation over K in Eq. (A1) *i.e.* it comes from the long-range part of the Coulomb interaction.

- ¹ P. K. Lam and S. M. Girvin, Phys. Rev. B **30**, R473 (1984); D. Levesque, J. J. Weis, and A. H. MacDonald, Phys. Rev. B **30**, R1056 (1984); K. Esfarjani and S. T. Chui, Phys. Rev. B **42**, 10758 (1990); K. Yang, F. D. M. Haldane, and E. H. Rezayi, Phys. Rev. B **64**, 081301(R) (2001); X. Zhu and S. G. Louie, Phys. Rev. B **52**, 5863 (1995).
- ² For recent reviews, see Physics of the electron solid, edited by S. T. Chui (International Press, Boston (1994) and H. Fertig and H. Shayegan in Perspectives in Quantum Hall Effects, edited by S. Das Sarma and A. Pinczuk (Wiley, New York, 1997), Chaps. 5 and 9 respectively.
- ³ P. D. Ye, L. W. Engel, D. C. Tsui, R. M. Lewis, L. N. Pfeiffer, and K. West, Phys. Rev. Lett. **89**, 176802 (2002).
- ⁴ Yong P. Chen, R. M. Lewis, L. W. Engel, D. C. Tsui, P. D. Ye, Z. H. Wang, L. N. Pfeiffer, and K. W. West, Phys. Rev. Lett. **93**, 206805, 2004.
- ⁵ Y. P. Chen, R. M. Lewis, L. W. Engel, D. C. Tsui, P. D. Ye, L. N. Pfeiffer, and K. W. West, Phys. Rev. Lett. **91**, 016801 (2003).
- ⁶ R. M. Lewis, Yong Chen, L. W. Engel, D. C. Tsui, P. D. Ye, L. N. Pfeiffer, and K. W. West, Physica E **22**, 104 (2004).
- ⁷ R. M. Lewis, P. D. Ye, L. W. Engel, D. C. Tsui, L. N. Pfeiffer, and K. W. West, Phys. Rev. Lett. **89**, 136804 (2002); R. M. Lewis, Y. Chen, L. W. Engel, D. C. Tsui, P. D. Ye, L. N. Pfeiffer, and K. W. West Phys. Rev. Lett. **93**, 176808 (2004); R. M. Lewis, Yong Chen, L. W. Engel, P. D. Ye, D. C. Tsui, L. N. Pfeiffer, and K. W. West, Physica E **22**, 119 (2004).
- ⁸ A. A. Koulakov, M. M. Fogler and B. I. Shklovskii, Phys. Rev. Lett. **76**, 499 (1996); M. M. Fogler, A. A. Koulakov, and B. I. Shklovskii, Phys. Rev. B **54**, 1853 (1996); R. Moessner and J.T. Chalker, Phys. Rev. B **54**, 5006 (1996); M. M. Fogler and A. A. Koulakov, Phys. Rev. B **55**, 9326 (1997). For a review of the bubble and stripe phases in higher Landau levels, see M. Fogler in High Magnetic Fields: Applications in Condensed Matter Physics and Spectroscopy, ed. by C. Berthier, L.-P. Levy, G. Martinez (Springer-Verlag, Berlin), 99 (2002).
- ⁹ Recently, Ettouhami et al. (cond-mat/0410343) considered the possibility that a class of distorted bubble states may exist in addition to those considered in this work. As the microscopic approach we use in this work does not appear to sustain states of this form, we do not consider their dynamical response in our study.
- ¹⁰ R. Côté, C. B. Doiron, J. Bourassa, and H. A. Fertig, Phys. Rev. B **68**, 155327 (2003).
- ¹¹ M.-R. Li, H. A. Fertig, R. Côté, and Hangmo Yi, Phys. Rev. Lett. **92**, 186804 (2004).
- ¹² Mei-Rong Li, H. A. Fertig, R. Côté, and Hangmo Yi, Phys. Rev. B (in press) (cond-mat/0409629).
- ¹³ M. Mézard, G. Parisi, and M. Virasoro, *Spin Glass Theory and Beyond* (World Scientific, Singapore, 1987); M. Mézard and G. Parisi, J. Phys. I **1**, 809 (1991); T. Giamarchi and P. Le Doussal, Phys. Rev. B **53**, 15206 (1996); T. Giamarchi and P. Le Doussal, Phys. Rev. B **52**, 1242 (1995); T. Giamarchi and E. Orignac, in *Theoretical Methods for Strongly Correlated Electrons*, CRM Series in Mathematical Physics (Spring, Berlin).
- ¹⁴ R. Chitra, T. Giamarchi, and P. Le Doussal, Phys. Rev. B **65**, 035312; *ibid.*, Phys. Rev. Lett. **80**, 3827 (1998); Chitra and Giamarchi, unpublished (cond-mat/0409187).
- ¹⁵ H. A. Fertig, Phys. Rev. B **59**, 2120 (1999).
- ¹⁶ H. Yi and H. A. Fertig, Phys. Rev. B **61**, 5311 (2000); M. M. Fogler and D. A. Huse, *ibid.* **62**, 7553 (2000).
- ¹⁷ L. D. Landau and E. M. Lifshitz, Theory of elasticity, Oxford, England, Pergamon Press (1986).
- ¹⁸ R. Côté, M.-R. Li, A. Faribault, H. A. Fertig, and Hangmo Yi, Proceedings of the 16th international conference on high magnetic fields in semiconductor physics, International Journal of Modern Physics B **18**, page (2004).
- ¹⁹ R. Côté and A.H. MacDonald, Phys. Rev. Lett. **65**, 2662 (1990); Phys. Rev. B **44**, 8759 (1991).
- ²⁰ L. Bonsall and A. A. Maradudin, Phys. Rev. B **15**, 1959 (1977).
- ²¹ V. Dotsenko, *Introduction to the Replica Theory of Disordered Statistical Systems*, Cambridge, New York (2001).
- ²² V. L. Berezinskii, Sov. Phys. JETP **38**, 620 (1974).
- ²³ See article by R. Kubo, S.J. Miyake, and N. Hashitsume, in *Solid State Physics* **17** (Academic Press, New York, 1965).
- ²⁴ M. P. Lilly, K. B. Cooper, J. P. Eisenstein, L. N. Pfeiffer and K. W. West, Phys. Rev. Lett. **82**, 394 (1999); R. R. Du, D. C. Tsui, H. L. Stormer, L. N. Pfeiffer, K. W. Baldwin and K. W. West, Solid State Comm. **109**, 389 (1999).
- ²⁵ N. Shibata and D. Yoshioka, Phys. Rev. Lett., **86**, 5755(2001); D. Yoshioka and N. Shibata, Physica A **12**, 43(2002).
- ²⁶ H. Fukuyama and P. A. Lee, Phys. Rev. B **18**, 6245 (1978).
- ²⁷ A.I. Larkin and Yu. N. Ovchinnikov, J. Low Temp. Phys. **34**, 409 (1979).
- ²⁸ W. Kohn, Phys. Rev. **123**, 1242 (1961).

²⁹ Hangmo Yi and H.A. Fertig, Phys. Rev. B **58**, 4019 (1998); R. Narevich, G. Murthy, and H.A. Fertig, Phys. Rev. B **64**, 245326 (2001); G.S. Geon, C.C. Chang, and J.K. Jain, cond-mat/0404747.

³⁰ C.C. Li, L.W. Engel, D. Shahar, D.C. Tsui, and M. Shayegan, Phys. Rev. Lett. **79**, 1353 (1997).

³¹ P.F. Hennigan, A. Beya, C.J. Mellor, R. Gaal, F.I.B. Williams, and M. Henini, Physica B **249-51**, 53 (1998).

³² B.G.A. Normand, P.B. Littlewood, and A.J. Millis, Phys. Rev. B **46**, 3920 (1992).